Appendix A: Comparison with other lines

In this section we present the comparison of the CO^+, [^{13}CII], ^{13}CO (10–9) and CO (9–8) line profile. Figure A.1 shows the CO^+ (in red), [^{13}CII] (Ossenkopf et al. 2013), ^{13}CO (10–9) and CO (9–8) lines (in black) at the IF position (Pilleri et al. 2012), with the intensity is scaled to unity. We find that CO^+ present larger linewidth than ^{13}CO and $H^{13}CO^+$ ($\approx$ 7 $\pm$ 0.7 km s^{-1}vs 3–5 km s^{-1}). Moreover, CO^+ line has a similar profile to that of the [^{13}CII] and CO line. The [^{13}CII] line presents its velocity peak at $\sim$9 km s^{-1}and the emission associated with the molecular gas (CO, ^{13}CO) is red-shifted, while the systemic velocity is $\sim$10 km s^{-1}.

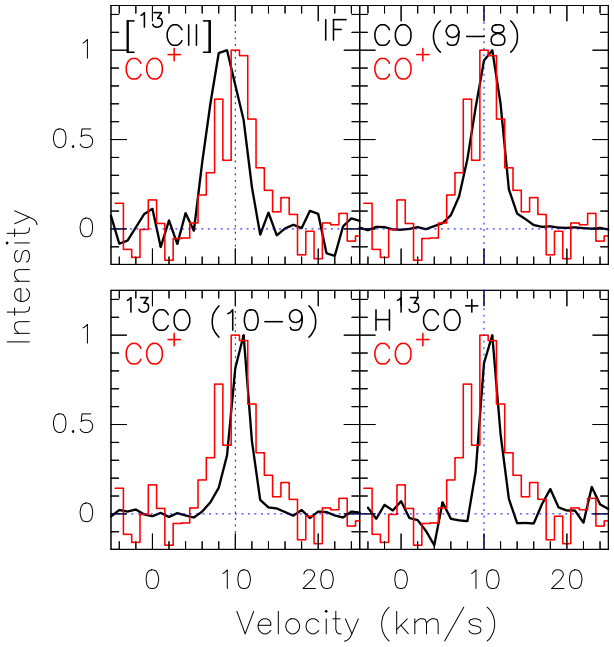

Fig. A.1. Comparison of the CO^+ line profile (in red) with the [^{13}CII], ^{13}CO (10–9), CO (9–8) and $H^{13}CO^+$ lines (in black) at the IF position, with the intensity is scaled to unity. *Herschel* data are presented in Pilleri et al. (2012) and Ossenkopf et al. (2013). The blue dotted line indicates the systemic velocity (10 km s^{-1}).

Appendix B: Column densities and fractional abundances

In this section we present the calculated CO^+, HCO^+ and C^+ column densities (N), as well as the fractional abundance $X(CO^+)$ of the IF, MP2 and PDR3 positions. The column densities were calculated in ranges of 1 km s^{-1}, from 5 km s^{-1} to 14 km s^{-1}. The CO^+ column densities have been calculated assuming a Boltzmann distribution of rotational levels with T_{ex} = 18 K. While for HCO^+ and C^+, we used RADEX and MADEX LVG codes (van der Tak et al. 2007 and Cernicharo 2012), considering the physical conditions derived by Berné et al. (2009). It is worth noting that for the IF position the HCO^+ emission is optically thick, thus we used the rarer isotopologue $H^{13}CO^+$ to correct the opacity effects and derive N[HCO^+] in each position, assuming $^{12}C/^{13}C$= 50 (Treviño-Morales et al. 2014). Regarding the N[C^+] estimation, we note that [CII] is optically thick towards the IF position (as seen by comparing the [CII] and [^{13}CII] lines): under the assumption of optically thin emission, [^{13}CII] results in a column density a factor 3–5 larger than that derived from the main isotopologue [CII]. From this, and considering that the other two positions are associated with less dense gas, we can infer that the assumption of optically thin emission applied to the [CII] in MP2 and PDR3, may underestimate the column density by a factor < 3. Because of the similar spatial distribution and velocity profiles between the CO^+ and C^+ we used N[C^+] to estimate the absolute fractional abundance $X(CO^+)$. For the calculations, we consider a beam filling factor of 1. This assumption is consistent with the fact that the beams of [CII] at 158μm, $H^{13}CO^+$ (3–2), HCO^+ (3–2) and CO^+ (2–1) are quite similar. Thus the calculated N[CO^+]/N[HCO^+] and X[CO^+] values are not affected by the beam filling factor. Table B.1 lists the calculated values of N[CO^+], X[CO^+], N[HCO^+], N[C^+] and N[CO^+]/N[HCO^+] in every velocity range.

Table B.1. Column densities and ratios, in ranges of 1 km s^{-1}, of the selected positions (see Fig. 2). We assumed LTE and T_{ex} = 18 K to calculate N[CO$^+$], while N[HCO$^+$] and N[C$^+$] have been calculated assuming LVG. For the IF position, we assume T_k = 600 K, $n_H = 4 \times 10^5$ cm^{-3}. For MP2 position, we assume T_k = 300 K and $n_H = 2 \times 10^5$ cm^{-3}. For PDR3 position, we assume T_k = 300 K and $n_H = 4 \times 10^4$ cm^{-3}.

Velocity range	(km s^{-1})	5 – 6	6 – 7	7 – 8	8 – 9	9 – 10	10 – 11	11 – 12	12 – 13	13 – 14	Total*
For the CO$^+$ line		$\sim 3\sigma$	$> 3\sigma$							$\sim 3\sigma$	
IF position — offset [0″, 0″]											
N[CO$^+$]	(in 10^{11} cm^{-2})	0.14	0.50	1.34	1.34	1.20	1.90	1.60	0.82	0.57	9.75[a]
N[HCO$^+$]	(in 10^{13} cm^{-2})	< 0.04	0.06	0.15	0.34	1.44	2.42	1.92	0.70	0.05	6.79[a]
N[C$^+$]	(in 10^{17} cm^{-2})	0.63	4.00	5.10	6.00	5.60	4.70	3.30	1.24	1.67	48.00[b]
N[CO$^+$]/N[HCO$^+$]		> 0.04	0.08	0.09	0.04	0.08	0.08	0.01	0.01	0.11	0.02
X[CO$^+$]	(in 10^{-11})	2.22	1.47	2.16	2.23	2.14	4.04	4.90	6.61	3.41	2.03
MP2 position — offset [0″, 40″]											
N[CO$^+$]	(in 10^{11} cm^{-2})	< 1.71	< 1.71	< 1.71	< 1.71	< 1.71	< 1.71	< 1.71	< 1.71	< 1.71	< 4.5[d]
N[HCO$^+$]	(in 10^{13} cm^{-2})	< 0.04	0.06	0.29	2.21	1.46	0.71	0.29	0.06	0.06	5.84[a]
N[C$^+$]	(in 10^{17} cm^{-2})	0.63	0.97	1.31	1.52	1.38	0.78	0.34	0.29	0.33	10.15[c]
N[CO$^+$]/N[HCO$^+$]		> 0.043	< 0.285	< 0.058	< 0.007	< 0.011	< 0.024	< 0.058	< 0.29	< 0.285	< 0.008
X[CO$^+$]	(in 10^{-10})	< 2.71	< 1.76	< 1.31	< 1.13	< 1.24	< 2.19	< 5.03	< 5.89	< 5.18	< 0.45
PDR3 position — offset [−10″, 24″]											
N[CO$^+$]	(in 10^{11} cm^{-2})	< 1.35	0.58	1.19	1.77	2.45	2.68	1.66	0.72	< 1.35	13.02[a]
N[HCO$^+$]	(in 10^{13} cm^{-2})	< 3.34	< 3.34	< 3.34	1.70	5.17	6.10	3.04	< 3.34	< 3.34	20.22[a]
N[C$^+$]	(in 10^{17} cm^{-2})	0.99	1.37	1.68	2.26	2.70	1.93	0.95	1.00	1.14	18.04[c]
N[CO$^+$]/N[HCO$^+$]		> 0.004	> 0.002	> 0.004	0.010	0.005	0.004	0.005	> 0.002	> 0.004	0.006
X[CO$^+$]	(in 10^{-10})	1.36	0.42	0.71	0.78	0.91	1.92	1.75	0.72	1.18	0.72

* Total velocity range of each line. [a] In a velocity range of 5 – 14 km s^{-1}. [b] In a velocity range of 4 – 25 km s^{-1}. [c] In a velocity range of 0 – 30 km s^{-1}. [d] considering the *rms* in a velocity range of 7 km s^{-1}.